Title
Infiltration of CD8 T Cells and Expression of PD-1 and PD-L1 in Synovial Sarcoma.

Journal
Cancer immunology research, 5(2)

ISSN
2326-6066

Authors
Nowicki, Theodore S
Akiyama, Ryan
Huang, Rong Rong
et al.

Publication Date
2017-02-01

DOI
10.1158/2326-6066.cir-16-0148

Peer reviewed

Research Article

Cancer Immunology Research

Infiltration of CD8 T Cells and Expression of PD-1 and PD-L1 in Synovial Sarcoma

Theodore S. Nowicki[1], Ryan Akiyama[1], Rong Rong Huang[2], I. Peter Shintaku[2], Xiaoyan Wang[3,4], Paul C. Tumeh[5,6,7], Arun Singh[8], Bartosz Chmielowski[9], Christopher Denny[1,7], Noah Federman[1,7,10], and Antoni Ribas[6,7,8,9]

Abstract

Tumors expressing programmed death ligand 1 (PD-L1) interact with the corresponding negative-signal generating immune receptor on the surface of CD8 T cells, PD-1, thereby suppressing antitumor activity. Therapeutics blocking this interaction have shown promise in various cancers by restoring functional antitumor T-cell activity. We explored the degree of PD-L1, PD-1, and CD8 expression in a retrospective analysis of 29 clinical synovial sarcoma samples. Quantitative immunohistochemistry and multiplex immunofluorescence were used to determine relative quantification of $CD8^+$ and PD-1^+ T cells and PD-L1 expression within the intratumor area and the interface between the tumor and the surrounding nontumor tissue (i.e., invasive margin), and colocalization of these factors, respectively. PD-L1, PD-1, and CD8 cell densities in the tumor-invasive margins were significantly higher in the metastatic tumors than the primary tumors ($P < 0.01$), and PD-L1, PD-1, and CD8 cell densities were all significantly positively correlated with one other ($P < 0.0001$). PD-1 cell density in the tumor-invasive margin was significantly associated with worse progression-free survival. Multiplex immunofluorescence demonstrated coexpression of PD-1 and CD8 on lymphocytes within the invasive margin, as well as relative proximity between PD-1^+ CD8 cells and PD-$L1^+$ tumor cells. Our results provide a preclinical rationale for screening of patients with synovial sarcoma for the colocalization of CD8, PD-1, and PD-L1, which may be a marker for response to PD-1 blockade therapy. *Cancer Immunol Res; 5(2); 1–11. ©2016 AACR.*

Introduction

Synovial sarcoma is an aggressive mesenchymal neoplasm with variable epithelial features, which accounts for 5% to 10% of all soft-tissue sarcomas (1). It chiefly affects older children and younger adults, and can occur at virtually any anatomic site. Clinical outcomes remain poor, with 5-year and 10-year survival rates of 60% and 50%, respectively (1, 2). Fifty percent of patients with synovial sarcoma patients develop metastases, primarily to the lungs or pleura, and have significantly worse clinical outcomes (1–3). Synovial sarcoma has a propensity for late recurrence and metastasis (occurring after 5 years), and 10 year minimum follow-up is generally recommended (1). Standard treatment for synovial sarcoma primarily consists of surgical resection, radiotherapy, and chemotherapy with alkylating agents, topoisomerase inhibitors, and anthracyclines. Although response rates of approximately 50% have been reported for these types of chemotherapy regimens, patients with refractory or recurrent/metastatic disease have few viable treatment options and none with proven improvements in survival (1, 2). The limitations in current treatment for synovial sarcoma make the development of new therapeutics a pressing concern, particularly for cases with metastatic disease.

The great majority (70%–80%) of synovial sarcomas express the cancer-testis antigen NY-ESO-1 (New York esophageal squamous cell carcinoma 1), which is encoded by the *CTAG1B* gene. This has allowed the successful clinical testing of a therapeutic approach targeting T cells specific for NY-ESO-1, with the use of adoptive cell therapy (ACT). ACT involves the generation of large quantities of CD8 T cells directed against specific tumor antigens. NY-ESO-1–specific T cells can be generated either by *ex vivo* expansion of endogenous, low-frequency NY-ESO-1–specific CD8 T cells, which are then re-infused into the patient (4, 5), or by *ex vivo* genetic modification of peripheral mononuclear blood cells, in which they are transduced with a T-cell receptor (TCR) directed against NY-ESO-1, expanded, and re-infused into the patient (6). Tumor vaccines have also been an effective means of stimulating patients' dendritic cells to help generate T-cell activity directed against NY-ESO-1 (7). Clinical trials involving NY-ESO-1–directed ACT against synovial sarcoma have shown promise in achieving objective clinical responses in patients with metastatic or refractory disease (6). These therapies, although not FDA-approved, are therefore increasingly attractive treatment choices

[1]Division of Pediatric Hematology-Oncology, Department of Pediatrics, University of California Los Angeles, Los Angeles, California. [2]Department of Pathology, University of California Los Angeles, Los Angeles, California. [3]Department of General Internal Medicine, University of California Los Angeles, Los Angeles, California. [4]Department of Health Services Research, University of California Los Angeles, Los Angeles, California [5]Division of Dermatology, Department of Medicine, University of California Los Angeles, Los Angeles, California. [6]Department of Molecular and Medical Pharmacology, University of California Los Angeles, Los Angeles, California. [7]Jonsson Comprehensive Cancer Center, Los Angeles, California. [8]Division of Hematology-Oncology, Department of Medicine, University of California Los Angeles, Los Angeles, California. [9]Division of Surgical-Oncology, Department of Surgery, University of California Los Angeles, Los Angeles, California. [10]Department of Orthopedics, David Geffen School of Medicine, University of California Los Angeles, Los Angeles, California.

Corresponding Author: Antoni Ribas, University of California Los Angeles, 11-934 Factor Building, 10833 Le Conte Avenue, Los Angeles, CA, 90095. Phone: 310-206-3928; Fax: 310-825-2493; E-mail: aribas@mednet.ucla.edu

doi: 10.1158/2326-6066.CIR-16-0148

for metastatic and refractory synovial sarcoma and underscore the inherent immunogenicity of this malignancy and the need to further enhance therapies that exploit this immunogenicity.

The experience with NY-ESO-1 ACT in synovial sarcoma highlights that this is a tumor type that can be targeted effectively with immunotherapies. It is possible that pre-existing T cells in synovial sarcomas could be inhibited by an immune checkpoint, and releasing this inhibitory signal may result in antitumor activity. Programmed cell death 1 (PD-1) and its corresponding ligand PD-L1 have emerged as important immune checkpoints by which cancer cells evade the host immune response. Under normal conditions, PD-1 is expressed on activated $CD8^+$ T cells, and its interaction with PD-L1 on host tissues leads to the inhibition of TCR signaling, limits the interactions between T cells and target cells, and ultimately leads to T-cell inactivation (8–11). PD-L1 expression is induced by localized inflammatory stimuli, such as IFNs, which are released by tumor-infiltrating lymphocytes (9). The PD-L1 induction process has been termed "adaptive immune resistance" (12) and represents a mechanism by which cancer cells protect themselves from immune-cell–mediated cell killing. This new paradigm led to the clinical development of antibodies blocking PD-1 or PD-L1, with which durable clinical responses are seen in a variety of malignancies, chiefly melanoma, non–small cell lung carcinoma, renal cell carcinoma, and diffuse large B-cell lymphoma (13–18). This has led to the exploration of the potential therapeutic utility of anti–PD-1/PD-L1 therapies in other malignancies as well. Previous work in other malignancies has explored how the presence of CD8 T cells in the tumor-invasive margin, along with concomitant PD-1 and PD-L1 expression within the tumor margin, predicts clinical response to PD-1 inhibitor therapy (19). Here, we report that PD-L1 expression is significantly increased in the invasive margin of metastatic synovial sarcoma tumors, and that this increased expression is correlated with significantly increased concentrations of PD-1 and $CD8^+$ T lymphocytes. Our data provide preclinical rationale for the utility of PD-1/PD-L1 inhibition as a therapeutic option in this malignancy.

Methods

Patients and samples

A retrospective cohort of patients with synovial sarcoma who had undergone surgical resection at UCLA Ronald Reagan and UCLA Santa Monica hospitals and had appropriate tumor tissue for analyses was selected for analysis following approval by the UCLA IRB (#15-001483). All cases chosen had previously been diagnosed as synovial sarcoma by pathologist interpretation and presence of SSX-S18 fusion oncogene via fluorescence ISH. Patient age at biopsy, gender, prior chemotherapy and/or radiotherapy, progression-free survival (PFS), and overall survival (OS) were recorded for subsequent statistical analysis. PFS was defined as time from biopsy to time of subsequent surveillance CT scan of chest/abdomen/pelvis demonstration progression of disease, or censored/lost to follow-up. OS was defined as time from biopsy to time of death or censored/lost to follow-up. For both PFS and OS, data were followed out to 60 months, beyond which they were censored. Formalin-fixed paraffin-embedded tissue blocks were obtained from the UCLA Translational Pathology Core Laboratory, and 5-μm-thick serial sections were generated for subsequent immunohistochemistry (IHC) and multiplex immunofluorescence.

Immunohistochemistry staining

Serial sections from patient tumor samples were stained for NY-ESO-1, PD-L1, PD-1, and CD8 at the UCLA Anatomic Pathology IHC Laboratory. Slides were deparaffinized and rehydrated with a series of graded ethanols to deionized water. Antigen retrieval was performed in Tris-EDTA at pH 9, and slides were cooked at high pressure at 120°C for 5 minutes. Immunostaining was performed on Leica Bond III autostainers using Leica Bond ancillary reagents (Leica Biosystems). Antibodies used included anti-CD8 clone C8/144B (1/100, DAKO), anti–PD-L1 clone SP142 (1/200, Spring-Bio), or anti–PD-1 clone NAT105 (1/50, Cell Marque). Antigen–antibody binding was visualized via the REFINE polymer 3,3′ diaminobenzidine (DAB) detection system (Lieca). Stained slides were treated with 0.5% cupric sulfate for 10 minutes, then counterstained with hematoxylin, and coverslipped for subsequent analysis.

Synovial sarcoma tumor marker immunostainings were performed manually. Antibodies used included anti–NY-ESO-1 clone E978 (1/200, pH 8 antigen retrieval, Santa Cruz Biotechnologies), anti–Bcl-2 clone 124 (1/300, pH 8 antigen retrieval; DAKO), anti-CD99 clone 12E7 (1/100, pH 8 antigen retrieval; DAKO), and anti-EMA clone E29 (1/500, pH 6 antigen retrieval; DAKO). For the Bcl-2, CD99, and EMA antibodies, antigen binding was again visualized via the REFINE polymer DAB detection system (Lieca). For the NY-ESO-1 antibody, antigen binding was visualized using biotinylated horse anti-mouse IgG antibody (Vector Laboratories), followed by agarose streptavidin (Vector Laboratories). DAB and hydrogen peroxide were used as the substrates for the peroxidase enzyme. All slides were counterstained with hematoxylin and coverslipped for subsequent analysis.

Digital image acquisition and analysis

All slides were scanned at an absolute magnification of 200X (0.5 μm/pixel) on an Aperio ScanScope XT system and imported for analysis using the Indica Labs Halo platform as previously described (19). Briefly, image analysis based on RGB (red, green, blue) spectra was used to detect all nucleated cells via counterstaining with hematoxylin. Areas were delineated as tumor margin via synovial sarcoma cell morphology, as well as the presence of positive staining for tumor markers Bcl-2, CD99, EMA, or NY-ESO-1 within serially stained sections. Following definition of tumor margin, concentric partitioning allowed the creation of a tumor perimeter of 400 μm, with 50% (200 μm) within the intratumor space, and 50% (200 μm) within the surrounding extra-tumor space. This area was defined as the invasive margin. Using the CytoNuclear module (cytoplasmic staining localization), algorithms were designed based on pattern recognition that were able to recognize positively stained NY-ESO-1, CD8, PD-1, or PD-L1 cells, and calculate the density (positive cells/mm^2) and percent cellularity (% positive cells/all nucleated cells) within both niches, except for NY-ESO-1, which was only calculated within the intratumor niche. Density and percent cellularity values for NY-ESO-1, CD8, PD-1, and PD-L1 stains all positively correlated with each other (r values of 0.89, 0.98, 0.98, and 0.97, respectively, $P < 0.0001$ for each), and density measurements were used for subsequent analyses.

Multiplex immunofluorescence

Multiplex immunofluorescence analysis was conducted on eight metastatic samples shown to display significant

expression of CD8, PD-1, and PD-L1. Serial sections from patient tumor samples were deparaffinized and rehydrated with a series of graded ethanols to deionized water. Antigen retrieval was performed in Tris-EDTA at pH 9, and slides were cooked at high pressure at 120°C for 15 minutes. Slides were then serially stained with anti–PD-1 clone NAT105 (1/1,500; Cell Marque), anti–PD-L1 clone SP142 (1/4,000; SpringBio), anti-CD8 clone C8/144B (1/5,000, DAKO), or anti-TLE1 clone ab183742 (1/2,000; Abcam), which served as a specific nuclear marker for synovial sarcoma tissue. Horseradish peroxidase–conjugated secondary labeling was performed using SuperPicture Polymer detection system. Signal for individual antibody complexes was labeled and visualized with FITC, Cy3, Cy5, and Cy3.5 tyramide signal amplification kits (PerkinElmer), individual primary/secondary antibody complexes were stripped via microwave treatment, and the process was repeated for each subsequent antibody labeling for a different antigen and fluorophore. Nuclei were visualized with Prolong Gold Antifade Reagent with DAPI (Invitrogen), and slides were then coverslipped for imaging. Stained slides were imaged using excitation and emission spectra for each individual fluorophore, and overlaid composite images were generated using the Vectra Intelligent Slide Analysis system on an Olympus BX-51WI microscope (PerkinElmer). Fields at 200X magnification were chosen which corresponded with areas of the invasive margin which were noted to have high expression of PD-L1, PD-1, and CD8 in the brightfield IHC experiments.

Statistical analysis

Descriptive statistics were calculated and presented in tables. For the comparison of the characteristics of primary patients and metastatic patients, unpaired Student t test was used for age, and the Fisher exact test was used for gender, prior chemotherapy, and prior radiotherapy. The OS probability and the PFS probability were estimated and presented by Kaplan–Meier survival curves. The log-rank test was used for testing the OS and the PFS between primary patients and metastatic patients, respectively. Differences between metastatic and primary tumors' PD-L1, PD-1, and CD8 brightfield IHC cell densities in intratumor and invasive margin niches were compared using the Wilcoxon rank-sum test, and correlations between PD-L1, PD-1, and CD8 cell densities were compared using Spearman rank correlation. For all subjects and the subsets of metastatic and primary tumors, univariate Cox proportional hazard regression was used to correlate OS/PFS with $\log_2$-transformed PD-L1, PD-1, and CD8 cell densities. All statistical tests were two-sided. P values less than 0.05 were considered statistically significant. Prism v6.0 software (GraphPad) and SAS Version 9.4 (SAS Institute, Inc.) were used for statistical analysis.

Results

Patient characteristics and clinical outcomes

Tumor tissues from biopsies and surgical resections from 29 patients with synovial sarcoma (12 primary lesions, 17 metastatic lesions) were selected for analysis. All metastatic samples were derived from lung metastases. Table 1 and Fig. 1A and B summarize data regarding the demographics, prior treatment, and PFS or OS between the two groups. At 60 months, the OS probabilities were 59.9% for all subjects, 78.6% for the patients with primary sarcoma, and 44.0% for the patients with metastatic sarcoma, respectively. The 60-month PFS probabilities were 53.3% for all subjects, 81.8% for the patients with primary sarcoma, and 34.3% for the patients with metastatic sarcoma, respectively. The metastatic disease population had a significantly higher incidence of prior chemotherapy than did the primary disease population.

PD-1 expression in tumor-invasive margins correlated with worse PFS survival

Biopsies were stained by IHC and analyzed using quantitative digital pathology via the Indica Labs Halo platform as described above (Fig. 2). PD-1 cell density in the invasive margin niche was significantly associated with worse PFS for all patients. The HR for $\log_2$-transformed PD-1 density in the invasive margin was 1.62 based on univariate Cox proportional hazard regression analysis ($P = 0.006$). CD8 and PD-L1 invasive margin cell densities approached, but did not achieve, statistically significant association with worse PFS, with HR values of 1.24 ($P = 0.082$) and 1.21 ($P = 0.071$), respectively. The association between CD8, PD-1, or PD-L1 intratumor cell densities and PFS was not statistically significant, nor was the association between CD8, PD-1, or PD-L1 invasive margin or intratumor cell densities and OS. No other associations were significant between CD8, PD-1, and PD-L1 densities in the invasive margin or the intratumor niches with patient age, gender, or prior treatment.

Metastatic synovial sarcomas had increased PD-L1, PD-1, and CD8 in invasive margins

Using the Halo image analysis platform to quantify cell densities within intratumor and invasive margin niches (data summarized in Table 2), we determined that PD-L1, PD-1, and CD8 cell densities in the tumor-invasive margins were all significantly higher in the metastatic tumors compared with the primary tumors (Fig. 3A). Furthermore, PD-L1, PD-1, and CD8 cell densities were all significantly positively correlated with one other within the invasive margin niche (Fig. 3B). Within the invasive margin niche, we observed positive correlation between cell density values for PD-1 with CD8 ($r = 0.76$, $P < 0.0001$), PD-L1 with CD8 ($r = 0.71$, $P < 0.0001$), and PD-L1 with

Table 1. Patient characteristics

Characteristic	Total ($N = 29$) patients (%)	Primary ($n = 12$) patients (%)	Metastatic ($n = 17$) patients (%)	Significance between primary and metastatic (P)
Gender				
Male	19 (65.6)	7 (58.3)	12 (70.6)	0.69
Female	10 (34.4)	5 (41.7)	5 (29.4)	
Mean age at surgery, years (interquartile range)	37.9 (25.0–48.0)	35.3 (24.5–46.0)	39.8 (28.0–49.0)	0.47
Prior chemotherapy	20 (69.0)	4 (33.3)	16 (94.1)	0.001
Prior radiotherapy	13 (41.4)	3 (25.0)	10 (5)	0.13

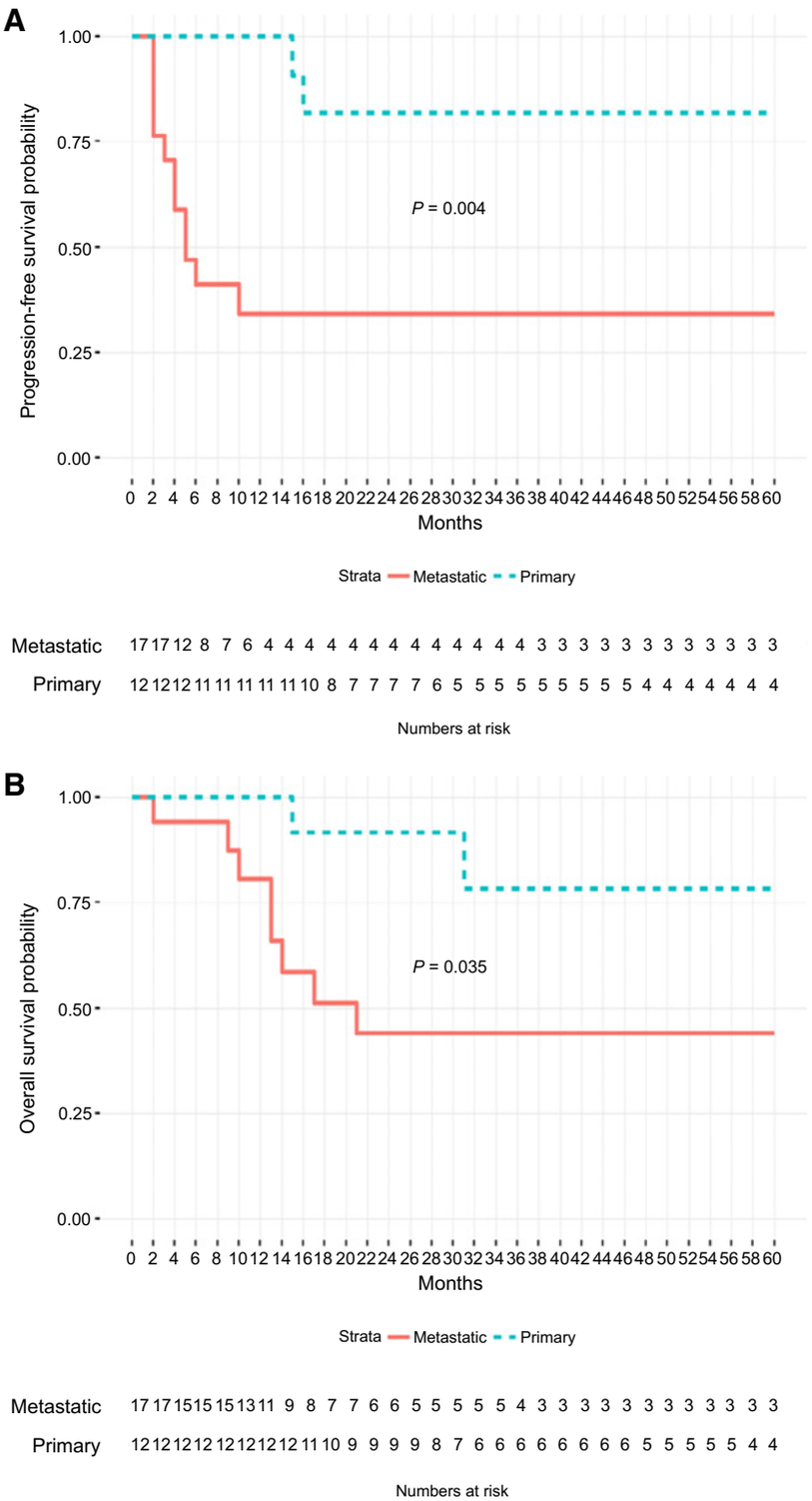

Figure 1.
Kaplan–Meier survival curves comparing PFS (**A**) and OS (**B**) between patients with primary and metastatic disease to 60 months.

PD-1 ($r = 0.67$, $P < 0.0001$). Intratumor PD-L1 density was also significantly higher ($P < 0.01$) in the metastatic tumors compared with the primary tumors (Fig. 3C). Although the CD8 and PD-1 cell densities trended higher in the intratumor niche of the metastatic tumors as compared with the primary tumors, the differences did not achieve statistical significance ($P = 0.11$ and $P = 0.08$, respectively). However, we still observed a similarly striking positive correlation between PD-1 with CD8 ($r = 0.72$, $P < 0.0001$), PD-L1 with CD8 ($r = 0.58$, $P < 0.01$), and PD-L1 with PD-1 ($r = 0.63$, $P < 0.001$) cell densities within the intratumor

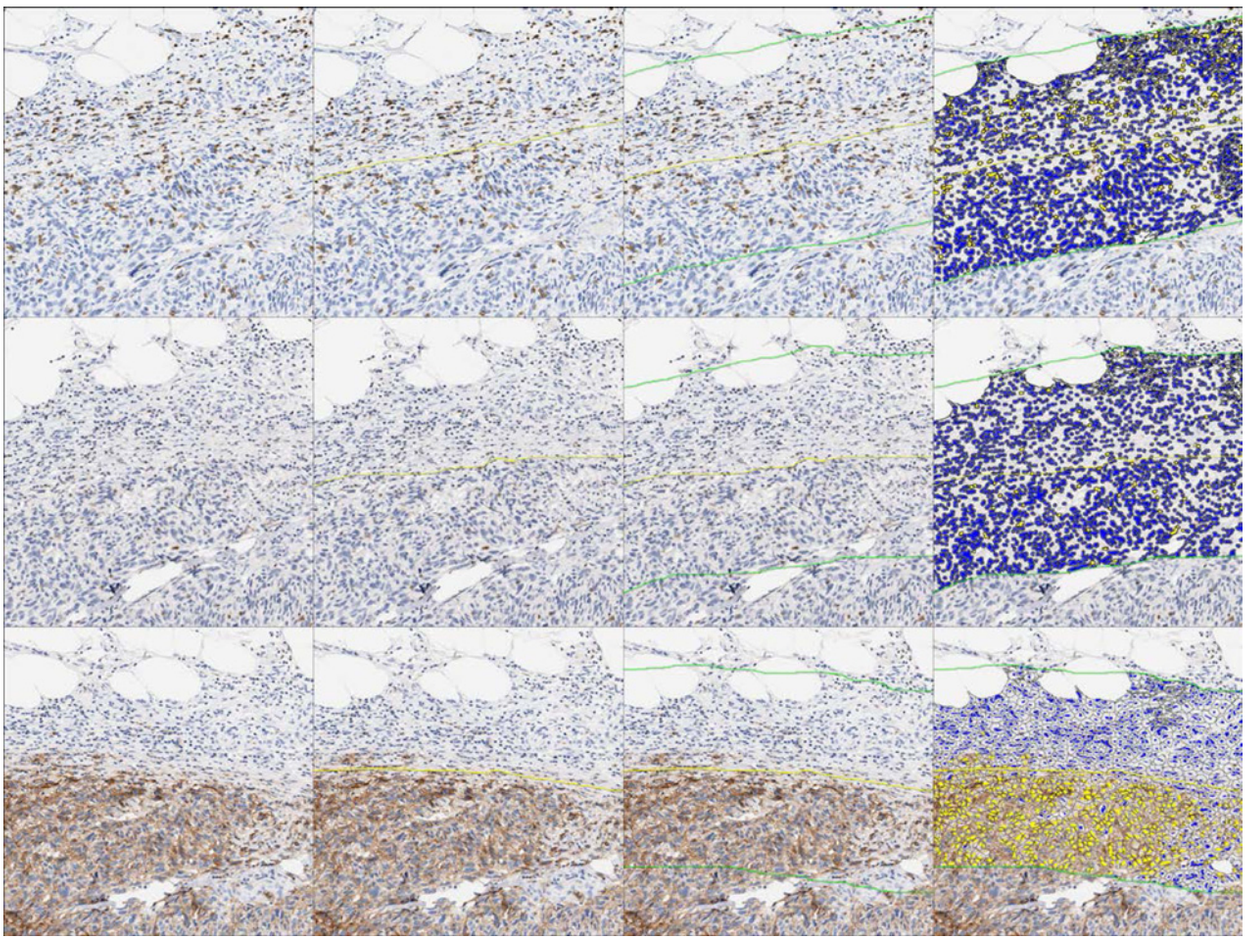

Figure 2.
Overview of quantitative IHC image analysis. Images represent the same fields of view of serial sections from tumor tissue. Tumor area (yellow line) is delineated via cell morphology and the presence of synovial sarcoma tumor markers in corresponding serial sections (Bcl-2, CD99, EMA, or NY-ESO-1). Once the tumor border has been established, a perimeter of 400-μm thickness is established via concentric partitioning, consisting of 50% intratumor space and 50% extra-tumor space. This perimeter (the area between the two green lines) is defined as the tumor-invasive margin. CD8, PD-1, and PD-L1 cell density analyses are then performed in serial sections for both the intratumor and the invasive margin niches, with cell density reported as number of positive cells/mm^2. Cells marked yellow are scored as positive, whereas cells marked blue are scored as negative. Magnification, ×80.

niche (Fig. 3D). NY-ESO-1 density was not correlated with CD8, PD-1, or PD-L1 densities in either the invasive margin or intratumor niches (data not shown).

Multiplex immunofluorescence was used to confirm that the increased PD-L1 and PD-1 expressions in the tumor-invasive margins were present on the synovial sarcoma tumor cells and the CD8 T cells, respectively. This technique enables the serial fluorescent labeling of multiple proteins within a single-tissue slide. Coexpression of PD-1 and CD8 was demonstrated on lymphocytes present within the tumor-invasive margins, as well as qualitative proximity between PD-1$^+$ cells and PD-L1$^+$ tumor cells. PD-L1 was expressed on tumor cells, which were distinguished by the presence of synovial sarcoma–specific TLE1 nuclear staining (Fig. 4).

Table 2. Summary of cell density measurements

Cell density	Total ($N = 29$) Mean, cells/mm^2; median, cells/mm^2 (range)	Primary ($n = 12$) Mean, cells/mm^2; median, cells/mm^2 (range)	Metastatic ($n = 17$) Mean, cells/mm^2; median, cells/mm^2 (range)	Significance between primary and metastatic (P)
CD8 (invasive margin)	107.9; 44.1 (0–730)	73.0; 9.9 (0–730)	132.5; 100.3 (23.1–357.1)	0.0003
PD-1 (invasive margin)	82.5; 48.9 (1.8–361.6)	41.6; 8.9 (1.8–293.2)	111.3; 83.4 (16.2–361.6)	0.002
PD-L1 (invasive margin)	174.2; 113.9 (0–1035)	80.0; 5.7 (0–862.8)	240.6; 194.5 (15.8–1,035)	0.0003
CD8 (intratumor)	53.4; 15.0 (1.3–414.3)	26.2; 8.1 (2.2–204.7)	72.6; 36.9 (1.3–414.3)	0.11
PD-1 (intratumor)	36.9; 11.1 (1.1–309)	24.8; 5.3 (1.1–182.9)	45.5; 20.9 (1.5–309)	0.08
PD-L1 (intratumor)	173.3; 24.3 (1.5–1,940)	171.3; 5.6 (1.5–1,940)	174.7; 53.7 (1.6–1,177)	0.006
NY-ESO-1	5,024; 5,334 (566–9,170)	4,682; 5,050 (566–8,693)	5,265; 5,920 (946–9,170)	0.44

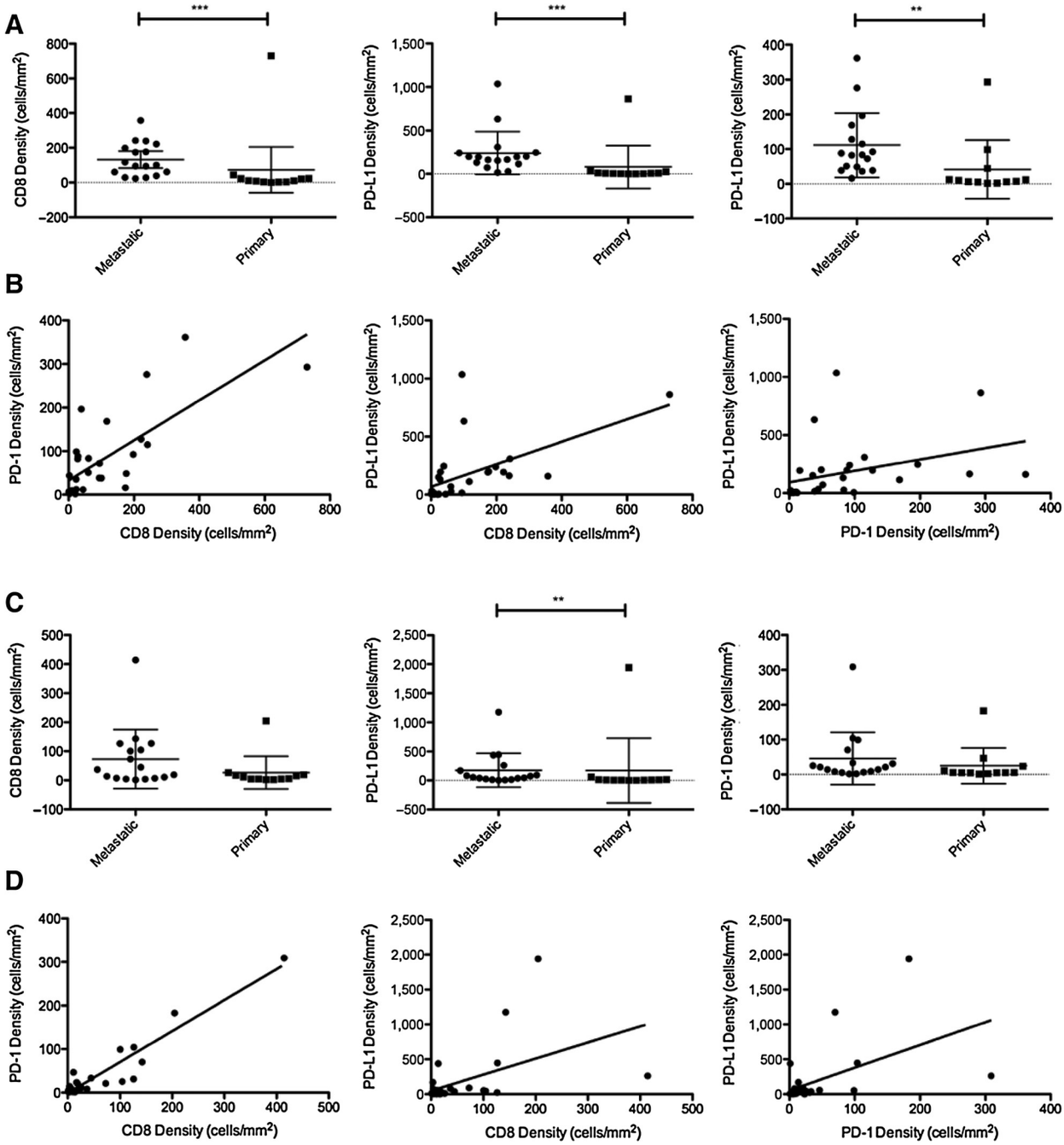

Figure 3.

A, Relative CD8, PD-L1, and PD-1 cell densities in the invasive margins of all samples of synovial sarcoma. PD-L1, PD-1, and CD8 cell densities were all significantly higher in the invasive margins of metastatic compared with primary tumors (**, $P < 0.01$; ***, $P < 0.0001$). Error bars represent SDs. **B,** Spearman correlation plots demonstrating that CD8, PD-L1, and PD-1 cell densities all positively correlate with one another within both the invasive margins. **C,** Relative CD8, PD-L1, and PD-1 cell densities in the intratumor margins of all samples of synovial sarcoma. PD-L1 cell densities were significantly higher in the intratumor niche of metastatic compared with primary tumors (**, $P < 0.01$). **D,** Spearman correlation plots demonstrating that CD8, PD-L1, and PD-1 cell densities all positively correlate with one another within the intratumor niches.

Discussion

Given the grim prognosis and lack of efficacious treatment options for metastatic synovial sarcoma, the exploration of novel therapeutics for this malignancy is of ample interest. The recent widespread success of T-cell–based immunotherapy for multiple other cancers, specifically via PD-1/PD-L1 inhibition, has

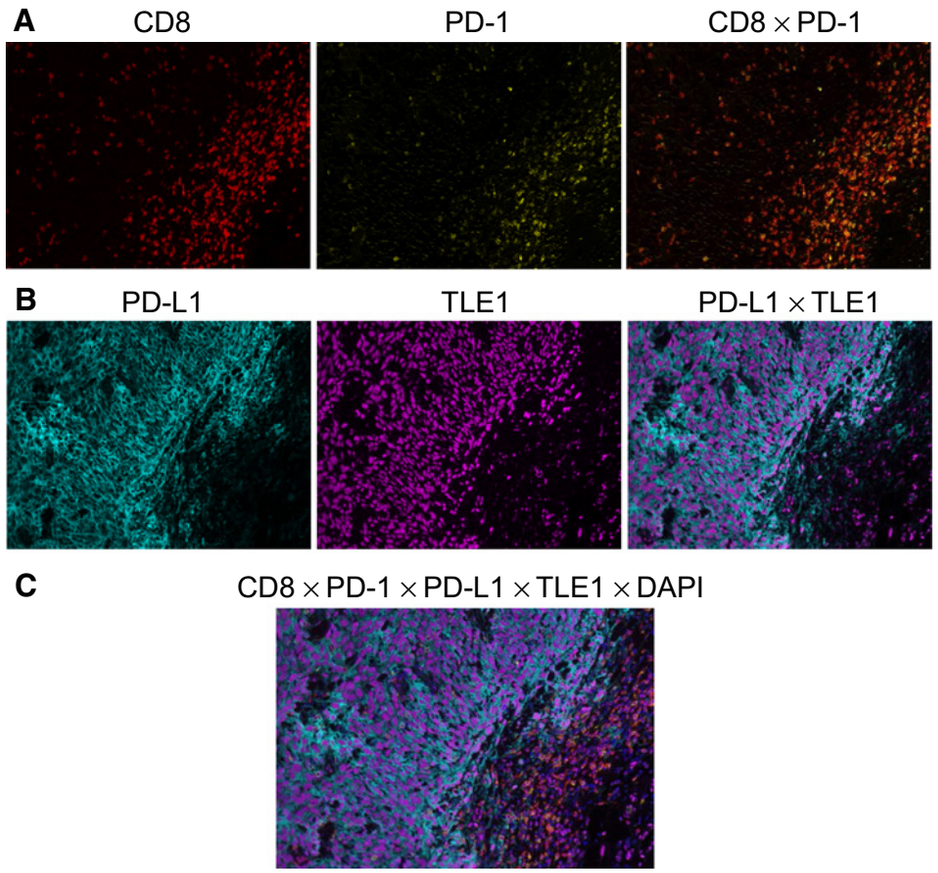

Figure 4.
Representative multiplex immunofluorescence image of synovial sarcoma with increased PD-L1/PD-1/CD8 cell densities at the tumor-invasive margin demonstrating colocalization of PD-1/CD8 double-positive lymphocytes with PD-L1/TLE1 double-positive synovial sarcoma cells at the invasive margin. Color scheme, Red: CD8, Yellow: PD-1, Cyan: PD-L1, Magenta: TLE1, Blue: DAPI. **A,** Coexpression of CD8 and PD-1 on lymphocytes (double positive = orange) concentrated at the invasive margin. **B,** Expression of PD-L1 by TLE1-positive synovial sarcoma cells at the invasive margin. **C,** Merged image of all labels. Magnification, ×200.

generated hope that these techniques could be applied to synovial sarcomas, as well as other soft-tissue malignancies.

Our data show that PD-L1 is expressed in synovial sarcoma, predominantly in lung metastases. This increased PD-L1 expression is proximally associated with increased concentrations of CD8 TILs expressing PD-1 in the tumor-invasive margin. It is known that PD-1 can be expressed on numerous cell types in addition to CD8 T cells, including B cells (20); PD-L1 expression has also been reported in dendritic cells, macrophages, plasma cells, and B cells (20–23). It is possible that the minority of cells observed expressing PD-L1 without TLE1, or PD-1 without CD8, may represent associated expression with any of these other cell types.

Our data showed that increased expressions of PD-L1, PD-1, and CD8 are directly correlated with one another. In several cases, PD-L1 expression was substantially higher than the associated PD-1 and CD8 expression densities (Fig. 3B and D). As PD-L1 can be either constitutively expressed or induced via localized inflammatory stimuli within the tumor microenvironment, such as IFNs (24–26), it may be that a subset of tumors have preexisting constitutive expression of PD-L1 in addition to induction by inflammatory stimuli. Alternatively, they may represent a subset of synovial sarcomas that are more sensitive to inflammatory stimuli, resulting in a more dramatic PD-L1 induction. Further studies at the genomic and transcriptomic levels are needed to fully elucidate the significance of such tumors as they pertain to potential responsiveness inflammatory stimuli and PD-1/PD-L1 inhibition.

These expression patterns of PD-L1 in close proximity to PD-1–positive CD8 TILs at the invasive margin are analogous to what our group has previously reported with melanoma (19), and what others have reported in other malignancies as well, including other sarcoma subtypes, such as gastrointestinal stromal tumors, osteosarcoma, and chondrosarcoma (25, 27–29). D'Angelo and colleagues previously reported a study of PD-L1, PD-1, and CD8 expression patterns in a large number of sarcoma subtypes (29). Although their study reported no significant expression of PD-L1, PD-1, or CD8 in synovial sarcoma, they only studied a very small number of samples from that malignancy ($n = 5$), their study did not distinguish between primary and metastatic tumor samples, and it did not specifically focus in the area of the tumor with most interest, the invasive margin. In our study, the higher incidence of prior chemotherapy was not associated with different PD-L1, PD-1, or CD8 expression. However, we found that PD-1 density in the tumor-invasive margin was significantly associated with lower PFS, and CD8 and PD-L1 densities in the invasive margin also approached significance in this association, as well. This phenomenon has been studied in multiple cancer subtypes, with PD-1 or PD-L1 expression levels being associated with either favorable or unfavorable impacts on PFS or OS, depending on the cancer type studied (30–33). Further prospective studies are needed to further explore and validate these associations, as well as further study how such expression patterns would predict responsiveness to PD-1/PD-L1 inhibitor therapy.

Given that our prior experience with melanoma demonstrated that the presence of CD8 TILs at the tumor-invasive margin (along

with concomitant proximal PD-1 and PD-L1 induction) predicted clinical response to PD-1 inhibition, it is reasonable to extrapolate that this pattern might predict clinical response to PD-1 inhibition in other tumor types as well. SARC 028 is an ongoing phase II clinical trial exploring the use of the pembrolizumab (an antibody to PD-1) in multiple sarcoma subtypes, including synovial sarcoma (34). It would be of great interest to correlate any clinical responses of synovial sarcoma patients with pre-existing CD8 infiltration and concomitant proximal PD-1 and PD-L1 expression. We have found no correlation between NY-ESO-1 density and CD8, PD-1, or PD-L1 density in either the invasive margin or intratumor niches. It may be that NY-ESO-1 is not a sufficiently strong enough antigen to provoke a significant CD8 T-cell response in itself. There may also be fundamental differences in certain subtypes of synovial sarcoma which render them more sensitive or resistant to a CD8 T-cell response. Spranger and colleagues previously reported an inverse relationship between melanoma-intrinsic β-catenin signaling and intratumoral T-cell infiltration (35, 36). Given that β-catenin induction has been documented in synovial sarcoma cases with particularly poor prognoses (37, 38), it may be that this or other factors may contribute to the baseline TIL activity which might be present in a given tumor. Further studies at the genomic and transcriptomic levels may reveal baseline tumor mutations, as well as novel tumor antigens or neoepitopes resulting from nonsynonymous mutations, which collectively are responsible for the immunogenicity of certain subsets of synovial sarcoma. However, a lack of pre-existing CD8, PD-1, or PD-L1 induction might not preclude the use of PD-1 inhibitors in synovial sarcoma, due to the high exploitability of this malignancy for adoptive cell therapy directed at NY-ESO-1. Patients without a pre-existing CD8 infiltrate could be provided one via adoptive cell therapy, which could then be combined with anti–PD-1 therapy to perpetuate the inherently limited duration of initially robust antitumor activity of this therapeutic modality. Alternatively, if endogenous T cells are already present in a given tumor, but their activation is blocked by PD-1/PD-L1 interactions, they may simply need to be unleashed *in situ*, as opposed to requiring the *ex vivo* manipulation of T cells.

Our study has several limitations. First, as our study was based on a retrospective analysis of synovial sarcoma tumors, we could not define a critical threshold of PD-L1, PD-1, or CD8 cell density required for a therapeutic response to PD-1/PD-L1 blockade. Additional studies in the future might identify expression thresholds linked to improved treatment responses. Furthermore, although the Aperio scans of the brightfield IHC slides enabled whole slide visualization with the ability to zoom in gradually up to 200x, the Vectra imaging system used for multiplex immunofluorescence imaging only permitted direct visualization using 200x total magnification. As such, we were unable to obtain whole slide images and subject them to the same whole slide analysis with the Indica Labs Halo platform that was used for the brightfield IHC. Finally, our analysis methods utilized serial slides derived from primary tumor resection or wedge resections of lung metastases of synovial sarcoma tumors instead of tissue microarrays, which we felt would not allow for accurate visualization of the tumor-invasive margin with the surrounding normal tissue. Although whole tumor or wedge resection analysis allows for a more complete representation of PD-L1, PD-1, or CD8 density variations within the tumor-invasive margin, we recognize that prospective wedge resection and subsequent analysis of lung metastases to determine likelihood of treatment success with PD-1/PD-L1 inhibitors may not be technically feasible in every patient.

In summary, our results provide preclinical rationale for screening of patients with synovial sarcoma for this pattern of PD-L1/PD-1 induction in the setting of CD8 T-cell infiltration, as well as possible treatment of patients with synovial sarcoma with PD-1/PD-L1 inhibitors, especially in patients with metastatic disease, who often have few treatment options. Patients who do not have a pre-existing CD8 infiltrate could potentially be given one via adoptive cell therapy, which could then be combined with PD-1/PD-L1 inhibition for enhanced therapeutic response.

Disclosure of Potential Conflicts of Interest

B. Chmielowski reports receiving honoraria from the Speakers Bureau of Genentech and is a consultant/advisory board member for BMS and Merck. No potential conflicts of interest were disclosed by the other authors.

Disclaimer

The contents of this article are solely the responsibility of the authors and do not necessarily represent the official view of the NIH, Stand Up To Cancer, or the Parker Institute for Cancer Immunotherapy.

Authors' Contributions

Conception and design: T.S. Nowicki, C. Denny, N. Federman, A. Ribas
Development of methodology: T.S. Nowicki, R.R. Huang, I.P. Shintaku, P.C. Tumeh, A. Ribas
Acquisition of data (provided animals, acquired and managed patients, provided facilities, etc.): T.S. Nowicki, R. Akiyama, R.R. Huang, I.P. Shintaku, P.C. Tumeh, A. Singh, B. Chmielowski, C. Denny, N. Federman, A. Ribas
Analysis and interpretation of data (e.g., statistical analysis, biostatistics, computational analysis): T.S. Nowicki, R. Akiyama, X. Wang, P.C. Tumeh, B. Chmielowski, A. Ribas
Writing, review, and/or revision of the manuscript: T.S. Nowicki, X. Wang, P.C. Tumeh, A. Singh, B. Chmielowski, N. Federman, A. Ribas
Administrative, technical, or material support (i.e., reporting or organizing data, constructing databases): R.R. Huang, A. Ribas
Study supervision: T.S. Nowicki, C. Denny, A. Ribas

Acknowledgments

We gratefully acknowledge the staff at the UCLA Translational Pathology Core Laboratories for technical assistance with tissue sample processing and digital slide image acquisition. We also gratefully acknowledge Philip Sanchez and Mariam Vanetsyan for their technical assistance and helpful conversations regarding the multiplex immunofluorescence image acquisition.

Grant Support

This work was funded by NIH grants R35 CA197633 and P01 CA168585, The Parker Institute for Cancer Immunotherapy, the Dr. Robert Vigen Memorial Fund, the Ressler Family Found, the Ruby Family Fund, the Wesley Coyle Memorial Fund, and the Garcia-Corsini Family Fund (to A. Ribas). A. Ribas was supported by a Stand Up To Cancer – Cancer Research Institute Cancer Immunology Dream Team Translational Research Grant (SU2C-AACR-DT1012). Stand Up To Cancer is a program of the Entertainment Industry Foundation administered by the American Association for Cancer Research.

The costs of publication of this article were defrayed in part by the payment of page charges. This article must therefore be hereby marked *advertisement* in accordance with 18 U.S.C. Section 1734 solely to indicate this fact.

Received June 30, 2016; revised November 1, 2016; accepted November 30, 2016; published OnlineFirst xx xx, xxxx.

References

1. Thway K, Fisher C. Synovial sarcoma: Defining features and diagnostic evolution. Ann Diagn Pathol 2014;18:369–80.
2. Krieg AH, Hefti F, Speth BM, Jundt G, Guillou L, Exner UG, et al. Synovial sarcomas usually metastasize after >5 years: A multicenter retrospective analysis with minimum follow-up of 10 years for survivors. Ann Oncol 2011;22:458–67.
3. Sandberg AA, Bridge JA. Updates on the cytogenetics and molecular genetics of bone and soft tissue tumors: Chondrosarcoma and other cartilaginous neoplasms. Cancer Genet Cytogenet 2003;143:1–31.
4. Pollack SM, Jones RL, Farrar EA, Lai IP, Lee SM, Cao J, et al. Tetramer guided, cell sorter assisted production of clinical grade autologous NY-ESO-1 specific CD8(+) T cells. J Immunother Cancer 2014;2:36.
5. Hunder NN, Wallen H, Cao J, Hendricks DW, Reilly JZ, Rodmyre R, et al. Treatment of metastatic melanoma with autologous CD4+ T cells against NY-ESO-1. N Engl J Med 2008;358:2698–703.
6. Robbins PF, Kassim SH, Tran TL, Crystal JS, Morgan RA, Feldman SA, et al. A pilot trial using lymphocytes genetically engineered with an NY-ESO-1-reactive T-cell receptor: Long-term follow-up and correlates with response. Clin Cancer Res 2015;21:1019–27.
7. Somaiah N, Block MS, Kim JW, Shapiro G, Hwu P, Eder JP, et al. Phase 1 first-in-human trial of LV305 in patients with advanced or metastatic cancer expressing NY-ESO-1. J Clin Oncol 2015;33:abstr 3021.
8. Ribas A. Tumor immunotherapy directed at PD-1. N Engl J Med 2012; 366:2517–9.
9. Keir ME, Liang SC, Guleria I, Latchman YE, Qipo A, Albacker LA, et al. Tissue expression of PD-L1 mediates peripheral T cell tolerance. J Exp Med 2006; 203:883–95.
10. Francisco LM, Sage PT, Sharpe AH. The PD-1 pathway in tolerance and autoimmunity. Immunol Rev 2010;236:219–42.
11. Fife BT, Pauken KE, Eagar TN, Obu T, Wu J, Tang Q, et al. Interactions between PD-1 and PD-L1 promote tolerance by blocking the TCR-induced stop signal. Nat Immunol 2009;10:1185–92.
12. Pardoll DM. The blockade of immune checkpoints in cancer immunotherapy. Nat Rev Cancer 2012;12:252–64.
13. Hamid O, Robert C, Daud A, Hodi FS, Hwu WJ, Kefford R, et al. Safety and tumor responses with lambrolizumab (anti-PD-1) in melanoma. N Engl J Med 2013;369:134–44.
14. Robert C, Ribas A, Wolchok JD, Hodi FS, Hamid O, Kefford R, et al. Anti-programmed-death-receptor-1 treatment with pembrolizumab in ipilimumab-refractory advanced melanoma: A randomised dose-comparison cohort of a phase 1 trial. Lancet 2014;384:1109–17.
15. Sundar R, Cho BC, Brahmer JR, Soo RA. Nivolumab in NSCLC: Latest evidence and clinical potential. Ther Adv Med Oncol 2015;7:85–96.
16. Topalian SL, Hodi FS, Brahmer JR, Gettinger SN, Smith DC, McDermott DF, et al. Safety, activity, and immune correlates of anti-PD-1 antibody in cancer. N Engl J Med 2012;366:2443–54.
17. Brahmer JR, Tykodi SS, Chow LQ, Hwu WJ, Topalian SL, Hwu P, et al. Safety and activity of anti-PD-L1 antibody in patients with advanced cancer. N Engl J Med 2012;366:2455–65.
18. Armand P, Nagler A, Weller EA, Devine SM, Avigan DE, Chen YB, et al. Disabling immune tolerance by programmed death-1 blockade with pidilizumab after autologous hematopoietic stem-cell transplantation for diffuse large B-cell lymphoma: Results of an international phase II trial. J Clin Oncol 2013;31:4199–206.
19. Tumeh PC, Harview CL, Yearley JH, Shintaku IP, Taylor EJ, Robert L, et al. PD-1 blockade induces responses by inhibiting adaptive immune resistance. Nature 2014;515:568–71.
20. Wlasiuk P, Niedzielski A, Skorka K, Karczmarczyk A, Zaleska J, Zajac M, et al. Accumulation of CD5+CD19+ B lymphocytes expressing PD-1 and PD-1L in hypertrophied pharyngeal tonsils. Clin Exp Med 2016;16:503–9.
21. Sponaas AM, Moharrami NN, Feyzi E, Standal T, Holth Rustad E, Waage A, et al. PDL1 expression on plasma and dendritic cells in myeloma bone marrow suggests benefit of targeted anti PD1-PDL1 therapy. PLoS One 2015;10:e0139867.
22. Parra ER, Behrens C, Rodriguez-Canales J, Lin HY, Mino B, Blando J, et al. Image analysis-based assessment of PD-L1 and tumor-associated immune cells density supports distinct intratumoral microenvironment groups in non-small cell lung carcinoma patients. Clin Cancer Res 2016;22:6278–89.
23. Qu QX, Huang Q, Shen Y, Zhu YB, Zhang XG. The increase of circulating PD-L1-expressing CD68(+) macrophage in ovarian cancer. Tumour Biol 2016;37:5031–7.
24. Bald T, Landsberg J, Lopez-Ramos D, Renn M, Glodde N, Jansen P, et al. Immune cell-poor melanomas benefit from PD-1 blockade after targeted type I IFN activation. Cancer Discov 2014;4:674–87.
25. Taube JM, Klein A, Brahmer JR, Xu H, Pan X, Kim JH, et al. Association of PD-1, PD-1 ligands, and other features of the tumor immune microenvironment with response to anti-PD-1 therapy. Clin Cancer Res 2014;20: 5064–74.
26. Spranger S, Spaapen RM, Zha Y, Williams J, Meng Y, Ha TT, et al. Up-regulation of PD-L1, IDO, and T(regs) in the melanoma tumor microenvironment is driven by CD8(+) T cells. Sci Transl Med 2013;5:200ra116.
27. Koirala P, Roth ME, Gill J, Piperdi S, Chinai JM, Geller DS, et al. Immune infiltration and PD-L1 expression in the tumor microenvironment are prognostic in osteosarcoma. Sci Rep 2016;6:30093.
28. Kostine M, Cleven AH, de Miranda NF, Italiano A, Cleton-Jansen AM, Bovee JV. Analysis of PD-L1, T-cell infiltrate and HLA expression in chondrosarcoma indicates potential for response to immunotherapy specifically in the dedifferentiated subtype. Mod Pathol 2016;29:1028–37.
29. D'Angelo SP, Shoushtari AN, Agaram NP, Kuk D, Qin LX, Carvajal RD, et al. Prevalence of tumor-infiltrating lymphocytes and PD-L1 expression in the soft tissue sarcoma microenvironment. Hum Pathol 2015;46:357–65.
30. Darb-Esfahani S, Kunze CA, Kulbe H, Sehouli J, Wienert S, Lindner J, et al. Prognostic impact of programmed cell death-1 (PD-1) and PD-ligand 1 (PD-L1) expression in cancer cells and tumor-infiltrating lymphocytes in ovarian high grade serous carcinoma. Oncotarget 2016;7:1486–99.
31. Wu P, Wu D, Li L, Chai Y, Huang J. PD-L1 and survival in solid tumors: A meta-analysis. PLoS One 2015;10:e0131403.
32. Muenst S, Soysal SD, Gao F, Obermann EC, Oertli D, Gillanders WE. The presence of programmed death 1 (PD-1)-positive tumor-infiltrating lymphocytes is associated with poor prognosis in human breast cancer. Breast Cancer Res Treat 2013;139:667–76.
33. Thompson RH, Dong H, Lohse CM, Leibovich BC, Blute ML, Cheville JC, et al. PD-1 is expressed by tumor-infiltrating immune cells and is associated with poor outcome for patients with renal cell carcinoma. Clin Cancer Res 2007;13:1757–61.
34. Burgess MA, Crowley J, Reinke DK, Riedel RF, George S, Movva S, et al. SARC 028: A phase II study of the anti-PD1 antibody pembrolizumab (P) in patients (Pts) with advanced sarcomas. J Clin Oncol 2015;33:abstr TPS10578.
35. Spranger S, Bao R, Gajewski TF. Melanoma-intrinsic beta-catenin signalling prevents anti-tumour immunity. Nature 2015;523:231–5.
36. Hu-Lieskovan S, Homet Moreno B, Ribas A. Excluding T cells: Is beta-catenin the full story? Cancer Cell 2015;27:749–50.
37. Barrott JJ, Illum BE, Jin H, Zhu JF, Mosbruger T, Monument MJ, et al. Beta-catenin stabilization enhances SS18-SSX2-driven synovial sarcomagenesis and blocks the mesenchymal to epithelial transition. Oncotarget 2015;6: 22758–66.
38. Trautmann M, Sievers E, Aretz S, Kindler D, Michels S, Friedrichs N, et al. SS18-SSX fusion protein-induced Wnt/beta-catenin signaling is a therapeutic target in synovial sarcoma. Oncogene 2014;33:5006–16.

AUTHOR QUERIES

AUTHOR PLEASE ANSWER ALL QUERIES

Q1: Page: 1: AU: Per journal style, genes, alleles, loci, and oncogenes are italicized; proteins are roman. Please check throughout to see that the words are styled correctly. AACR journals have developed explicit instructions about reporting results from experiments involving the use of animal models as well as the use of approved gene and protein nomenclature at their first mention in the manuscript. Please review the instructions at http://www.aacrjournals.org/site/InstrAuthors/ifora.xhtml#genenomen to ensure that your article is in compliance. If your article is not in compliance, please make the appropriate changes in your proof.

Q2: Page: 1: Author: Please verify the drug names and their dosages used in the article.

Q3: Page: 1: Author: Please verify the affiliations and their corresponding author links.

Q4: Page: 1: Author: Please verify the corresponding author details.

Q5: Page: 1: Author: Please check the sentence "Quantitative immunohistochemistry and multiplex immunofluorescence. . ." for sense.

Q6: Page: 2: Author/PE: Should the head "Methods" be changed to "Materials and Methods"?

Q7: Page: 2: Author: Please define "UCLA IRB."

Q8: Page: 2: Author: Please check the sentence "PFS was defined as time from biopsy to time of subsequent. . ." for sense.

Q9: Page: 2: Author: Please verify the change of "micron" to "μm" in the text for correctness.

Q10: Page: 3: Author: Please verify the layout of Tables 1 and 2 for correctness.

Q11: Page: 4: Author: Please confirm quality/labeling of all images included within this article. Thank you.

Q12: Page: 8: AU:/PE: The conflict-of-interest disclosure statement that appears in the proof incorporates the information from forms completed and signed off on by each individual author. No factual changes can be made to disclosure information at the proof stage. However, typographical errors or misspelling of author names should be noted on the proof and will be corrected before publication. Please note if any such errors need to be corrected. Is the disclosure statement correct?

Q13: Page: 8: Author: Please verify the heading "Disclaimer" and its content for correctness.

Q14: Page: 8: Author: The contribution(s) of each author are listed in the proof under the heading "Authors' Contributions." These contributions are derived from forms completed and signed off on by each individual author. As the corresponding author, you are permitted to make changes to your own contributions. However, because all authors submit their contributions individually, you are not permitted to make changes in the contributions listed for any other authors. If you feel strongly that an error is being made,

then you may ask the author or authors in question to contact us about making the changes. Please note, however, that the manuscript would be held from further processing until this issue is resolved.

Q15: Page: 8: Author: Please verify the headings "Acknowledgments" and "Grant Support" and their content for correctness.

AU: Below is a summary of the name segmentation for the authors according to our records. The First Name and the Surname data will be provided to PubMed when the article is indexed for searching. Please check each name carefully and verify that the First Name and Surname are correct. If a name is not segmented correctly, please write the correct First Name and Surname on this page and return it with your proofs. If no changes are made to this list, we will assume that the names are segmented correctly, and the names will be indexed as is by PubMed and other indexing services.

First Name	**Surname**
Theodore S.	Nowicki
Ryan	Akiyama
Rong Rong	Huang
I. Peter	Shintaku
Xiaoyan	Wang
Paul C.	Tumeh
Arun	Singh
Bartosz	Chmielowski
Christopher	Denny
Noah	Federman
Antoni	Ribas